



# Unraveling the structural, electronic and magnetic properties of $\text{Mn}_1\text{Pd}_{n-1}$ , $\text{Mn}_2\text{Pd}_{n-2}$ and $\text{Pd}_n$ ( $n=13$ ) clusters

G. C. Kaphle \* and N. P. Adhikari

Central Department of Physics, Tribhuvan University, Kirtipur, Kathmandu, Nepal

\* Email: [gopi.kaphle@cdp.tu.edu.np](mailto:gopi.kaphle@cdp.tu.edu.np)

Received: 3<sup>rd</sup> May, 2023; Revised: 25<sup>th</sup> June, 2023; Accepted: 9<sup>th</sup> August, 2023

## Abstract

This work presents a systematic study of the geometric, electronic and magnetic properties of Pd clusters pristine and mono- and bi-doped with Mn:  $\text{Pd}_n$ ,  $\text{Pd}_{n-1}\text{Mn}$ ,  $\text{Pd}_{n-2}\text{Mn}_2$  where  $n \leq 13$ . We have used the density functional formalism with the spin polarized generalized gradient approximation. From the variety of possible structures with thirteen atoms, we found the icosahedral configuration to be the most stable as compared to the hexagonal, cub-octahedral and buckled bi-planar. The change in magnetic behavior of Pd clusters after doping with Mn has been observed. This communication is an attempt to understand that behaviour.

**Keywords:** clusters, SPGGA, stable conformer, doping, magnetism.

## Introduction

Atomic and molecular clusters have a wide variety of potential and actual technological uses (Bansmann et al, 2005). A large number of research exists on clusters. Technologically, transition metal clusters (TMC) serve as catalysts in many industrial and important chemical processes (Kumar and Kawazoe 2002, 2003). They are also used extensively in sensing devices, magnetic storage material and constitute important components in nanomaterials for diverse applications. TMC exhibit wide variety of geometric isomers and shapes. The physico-chemical properties of these clusters critically depend upon their size and shapes dictated by their atomic arrangements. So understanding the evolution of these properties of clusters with size is necessary for the design and development of novel materials (Kumar & Kawazoe 2006, 2001).

Pd clusters serve as excellent catalysts in many heterogeneous catalytic systems (Aguilera-Granja et al. 2004). They exhibit interesting magnetic properties and show promise for essential application as supported metal catalysts. The magnetic properties of these catalysts are determined by their electronic structures and ultimately by their atomic arrangement (Shinohara et al. 2003). From earlier studies, it is known that even a 6% increment in the lattice constant can cause magnetism to appear in the system. In general, as size decreases, by the Stoner argument, magnetic moment approaches the atomic value in a magnetic material (Zhang et al. 2008; Luo et al. 2007). This is usually higher than in the bulk.

The Pd atom is non-magnetic with a closed shell electronic configuration,  $4d^{10} 5s^0$ . But in the small cluster, interaction between Pd atoms involves s, p, d hybridization, which leads to the depletion of 4d electrons and hence give rise to local magnetic moments (Rogan et al. 2008, Aguilera-Granja 2009). There are many conflicting remarks from both experimental and theoretical studies regarding the magnetic moments of small size Pd clusters (Chang & Chou 2004) Stern-Garlach experiments suggested that there was no net magnetic moment in Pd clusters (Chen et al. 2006; Huber & Herzberg 1979), whereas photoemission studies proposed that in smaller clusters, with less than 15 atoms, there was a finite magnetic moment (Nigam et al. 2007; Massen et al. 2002). However the experimental study of Taniyama et.al. (Taniyama, Ohta, & Sato 1997) reported net magnetic moments even in the larger size Pd clusters. From theoretical studies, Moseler et.al. (Moseler et al. 2001) reported that all small clusters  $\text{Pd}_n$  ( $n=2-7$  and 13) exhibit a finite magnetic

moment. Similar arguments have been made by Kumar and Kawazoe (Kumar & Kawazoe 2001, 2002) and Lee et.al. (Lee & Chang 2011). Reddy et.al. (Reddy et al. 1993, 1933) performed a calculation of the electronic structure of a 13-atom cluster of 4d group elements using local spin density approximation and reported that an icosahedron isomer of Pd 13 has a stable structure with large magnetic moment. Nigam et.al. (Nigam et al. 2007, Mu et al. 20011) studied the geometrical, electrical and magnetic properties of Pd clusters doped with other transition metals. They reported that Mn, Fe and Co enhance the magnetic moments of Pd clusters due to ferromagnetic coupling and  $\text{Pd}_{12}\text{Mn}$  carries magnetic moment about  $11\mu_B$ . Chang and Chou (Chang & Chou 2004) reported that new types of structures called buckled bi-planer (BPP) with  $C_{2v}$  symmetry have lower energy than that of icosahedral and cub-octahedral clusters. They claimed that BPP is the lowest energy structure and this trend is followed by all transition elements with more than half fulfilled d-shells (Blonski & Hafner 2011).

The motivation for this work is twofold: first, to have a fresh look at the body of, often, contradictory results and, by carrying out a systematic study, remove these uncertainties. Secondly, to understand the influence of Mn impurities on the electronic, atomic and magnetic structure of host Pd cluster. In present work we study, in particular, the structure, density of states and magnetic properties of different isomers of  $\text{Pd}_{13}$ ,  $\text{MnPd}_{12}$  and  $\text{Mn}_2\text{Pd}_{11}$  in some detail. The rest of the paper is organized as follows: The computational details and theoretical background for the calculations are described in Section 2 after the introduction. The result of the present work has been described in Section 3 which are discussed and analyzed in Section 4. Finally Section 5 consists of concluding remarks of the present work.

## Computational details and theoretical background

The density functional theory (DFT) with the projected augmented wave (PAW) formulation has been used for the calculation of total energy and geometrical optimization of clusters through Vienna ab initio simulation package (VASP) (Kresse & Joubert, 1999; Kresse & Frauhoffer, 1996). Spin-polarized generalized gradient approximation (GGA) has been used for the calculation of exchange correlation energy (Perdew, Burke & Ernzerhof 1996). The spin states and magnetic moments were then determined based on the calculated energies of spin up and spin down orbitals. The kinetic energy cut off used were maximal default values recommended by the pseudo-potential database, i.e. 250 eV for Pd n clusters and 400 eV for

$Pd_nMn$  and  $Pd_nMn_2$  clusters. A simple cubic super-cell with side dimension  $16\text{\AA}$  was used in the calculation. A single  $\Gamma$  point integration was carried out over the Brillouin zone and all the atoms were allowed to relax following Hellman-Feynman forces on each atom until the force became less than  $0.01\text{ eV/\AA}$  and energy has converged to an accuracy of  $0.001\text{ eV}$ . In order to check the reliability of pseudo-potential used in the present work, test calculations were performed for bulk Pd and PdMn, and the lattice constants ( $2.56\text{\AA}$  and  $3.65\text{\AA}$ ) and cohesive energies were found to be in fair agreement with experimental results (Piotrowski, Piquini & Da Silva, 2010; Castleman & Jena 2006; Alonso 2000).

All the cluster geometries were fully optimized without imposing symmetry constraints except for the icosahedral structure for which point group symmetries were utilized to simplify the calculation. The average binding energy of the cluster was calculated using the formula:

$$E_B(Pd_nX_m) = [nE(Pd) + mE(X) - E(Pd_nX_m)] / (n+m) \quad (1)$$

where  $E(Pd_nX_m)$ ,  $E(X)$  and  $E(Pd)$  are the total energies of  $Pd_nX_m$ , X and Pd respectively.

The relative stability of cluster against the loss of one of its constituent's atoms is called the dissociation energy.

We define this quantity for Pd and mono and bi-doped Pd clusters as:

$$\Delta_1(Pd_nX_m) = E(Pd_n) + mE(X) - E(Pd_nX_m) \quad (2)$$

where all symbols have their usual meanings.

The second difference of total energy gives the enhanced stability of a cluster, relative to its heavier and lighter neighbors, which can be calculated using the formulae,  $\Delta_2(Pd_nX_m) = E(Pd_{n-1}X_m) + E(Pd_{n+1}X_m) - 2E(Pd_nX_m)$  (3)

The values of  $\Delta_1$  and  $\Delta_2$  have local structure, but generally decrease slowly as co-ordination increases with the size of cluster.

In order to get the knowledge of magnetic stability of any cluster we have to analyze the spin-gaps, which are defined as:

$$\delta_1 = -[\epsilon_{HOMO}^{Majority} - \epsilon_{LUMO}^{Minority}] \quad (4)$$

The cluster is said to be stable if both the spin gaps are positive i.e. the lowest unoccupied molecular orbitals (LUMO) of majority spin lies above the highest occupied molecular orbital (HUMO) of minority spin and vice versa.

### III. RESULTS AND DISCUSSION

#### A: STRUCTURAL EFFECTS OF DOPING

To begin with we shall study the pristine Pd clusters up to a size of 13 atoms. This will form the background of our doping studies. It was necessary to describe the pristine clusters using exactly the same methodology and parameters as the later doping studies, so that a consistent picture emerges.

We have carried out full structural optimization for all sizes. Leftmost figures in Fig.1 show the optimized structures for pristine Pd clusters with  $n = 1-13$ . For the 13 atom cluster we find the icosahedral isomer to be of the lowest energy rather than the BBP as suggested earlier. The various isomers are shown in Fig.2. Next we shall optimize the mono-doped and bi-doped clusters taking

into account possible isomers. Fig.1 shows the lowest energy isomers for each size.

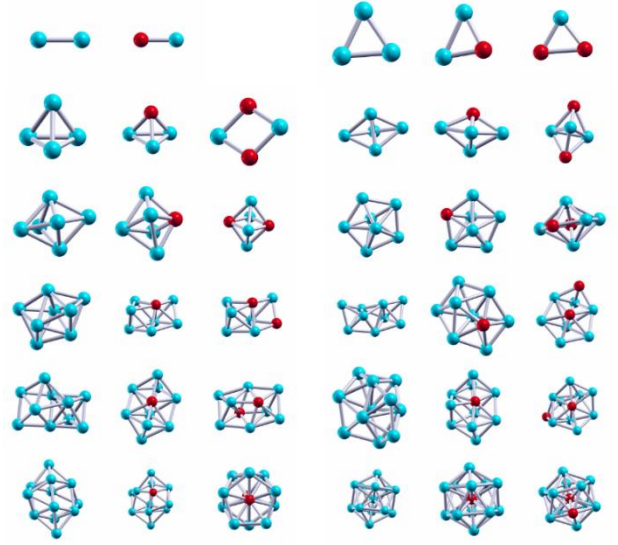


FIG. 1. The lowest energy configurations for pristine Pd clusters and Pd clusters mono-doped and bi-doped of Mn with cluster sizes varying from two to thirteen.

We have compared the doped with the pristine clusters. Our conclusions are described below:

- (i) For  $Pd_2$  the bond length is found to be  $2.48\text{\AA}$  not very different than the experimental value of  $2.52\text{\AA}$ . This agrees with earlier work as well. The  $PdMn$  cluster has a bond length of  $2.25\text{\AA}$ , which is consistent with the stronger binding between Pd and Mn as compared with between two Pd atoms.
- (ii) For  $Pd_3$  the stable structure is the isosceles triangle. The expected equilateral triangle is distorted due to Jahn-Teller effect. The linear structure is higher in energy by about  $0.4\text{ eV/atom}$ . The stable structure for  $Pd_2Mn$  is also isosceles from symmetry considerations. The average bond length is  $2.51\text{\AA}$  while the Pd-Mn bonds lengths are  $2.45\text{\AA}$ . Again this is consistent with the stronger Pd-Mn bonding. The  $PdMn_2$  cluster has an average bond length of  $2.49\text{\AA}$ . This is indicative of stronger Pd-Mn and Mn-Mn bonding. In all three cases the linear configuration is higher in energy and therefore unstable.
- (iii) The lowest energy stable structure for  $Pd_4$  is the tetrahedron while that for  $Pd_3Mn$  is a distorted tetrahedron with Pd-Pd bond lengths larger than Pd-Mn ones. For the  $Pd_2Mn_2$  the planar rhombus with Mn atoms at two opposite ends wins over three dimensional isomers. This resembles the planar structures found in pristine Mn clusters and may therefore be associated with co-ordination related to Mn.
- (iv) Clusters of sizes 5-7 all grow in bi-pyramidal configurations with increasing bond length and binding energies. The Mn atoms are directly bonded with four Pd atoms and for the bi-doped clusters the Mn atoms sit on opposite corners. The three dimensional structures win over those with planer geometry. As the size increases, the number of isomers also increase. The difference in binding energies among the isomers is rather small and when such clusters are formed at finite temperatures the isomers may also be present.

- (v)  $Pd_8$  lowest energy structure is a distorted bi-pyramid and appears to be quite “irregular”. The configuration with distorted double octahedron with one facet is most stable. The doped clusters resemble the pristine one with the expected distortions around the Mn sites.
- (vi) The structure of pristine  $Pd_9$  is a distorted half-icosahedron. But the doped clusters have characteristic icosahedral signatures which do not resemble the pristine clusters.
- (vii) Earlier works reported that for pristine  $Pd_{10}$  the most stable structure was the bi-capped octahedron. We find this to be a near energy isomer. The stable structure is a distorted irregular structure. The mono-doped  $Pd_9Mn$  is a square bi-pyramid with Mn at one of the square bases while the bi-doped  $Pd_8Mn_2$  is a double pentagon. These doped clusters resemble neither the pristine Pd cluster nor each other.
- (viii) For  $Pd_{11}$  structure with the highest binding energy has three octahedrons each of which fuses one facet with the other two having average bond length  $3.63\text{\AA}$ .  $Pd_{10}Mn$  has icosahedral while  $Pd_9Mn_2$  bears a cubo-octahedral signature. Again these doped clusters resemble neither the pristine Pd cluster nor each other.
- (ix) For  $Pd_{12}$  we deal with two almost degenerate isomers: the cub-octahedron and the icosahedron with vacant centers. The cub-octahedron with a vacant central atom has  $0.014\text{ meV}$  lower binding energy than the icosahedral. This energy difference is within our error bar of calculations, so we cannot decide between these isomers with any confidence. Now both the mono and bi-doped clusters resemble the pristine one.
- (x) For  $Pd_{13}$  a typical icosahedral structure with binding energy  $2.311\text{ meV}$  is found to be most stable. Chang and Chau suggested that then buckled biplaner structure could be the ground state. In present work we observed that the icosahedral structure has  $0.007\text{ eV}$  lower bonding energy as compared to the buckled biplaner structure.

Our results are consistent with other theoretical works (Aguilera-Granja, 2004). Both the mono- and bi-doped clusters have icosahedral signatures. The isomers are shown in Fig. 2. The Fig. 3 and Table I summarizes all the characteristics of pristine Pd clusters with binding energies, energy differences, magnetic moments, bond lengths and spin-gaps. This will now form the basic cluster in which Mn atoms will be doped.

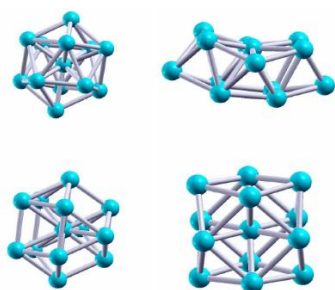


FIG. 2. The different isomers of  $Pd_{13}$  clusters Doping of Pd clusters with different atoms like Mn is expected to open up other channels where in one can tailor the properties of clusters by varying the nature of doping.

Large magnetic moments in Mn substitutional doped Pd 13 clusters have been predicted, so it is of great interest to study the effect of Mn doping on Pd clusters. Bulk Pd alloyed with Mn undergo paramagnetic to ferromagnetic and also anti-ferromagnetic and spin-glass transitions in some regions of the composition-temperature phase diagram. It would be rather interesting to know how Mn doping influences the magnetic behavior of Pd clusters. We shall address this problem in the next two sections.

### Binding and stability

In this section we shall focus on the binding and stability of Pd  $n$  clusters and the effect of doping on these properties. The Fig. 3 shows the binding energies, the first difference (dissociation energy) and the second difference energies together with the spin-gaps as functions of cluster size.

For the pristine Pd clusters, binding energy (BE) increases monotonically with cluster size and tends towards the bulk cohesive energy  $3.89\text{ eV/atom}$  of bulk Pd solid. This is also true for the doped clusters. Higher binding energy reflects greater stability. Hence our study indicates that from Fig. 3 top left panel that stability increases with number of Mn atoms doped for all cluster sizes. This indicates that enhancement of stability arises mainly comes from the doping of Mn the Pd clusters. From Fig. 4 we observed that Pd-Pd and Pd-Mn bond lengths increase on doping.

There is transfer of electrons from Mn to Pd due to their different electro-negativities ( $1.55$  for Mn and  $2.20$  for Pd). The Fig. 4 shows the charge transfer is greater for most sizes for the mono-doped as compared to the bi-doped clusters. There is a clear correlation between shorter bond lengths and stronger ionic type bonding related to charge transfer (Grune et al. 2008) In order to get a clear picture of stability let us analyze the dissociation energy and second difference energy in greater detail. The peaks of the dissociation energy represent greater stability. The pristine Pd clusters show odd-even alternation up to  $n = 6$  and show peaks  $n = 8, 10$  and  $13$  indicating that clusters of these sizes were more stable as compare to their neighbors. This follows magic number sequence. In case of mono-doped Pd clusters  $Pd_2Mn, Pd_4Mn, Pd_7Mn$  and  $Pd_{12}Mn$  show peaks indicating that they were more stable than their neighbors. Similarly more stable clusters in the bi-doped series were at  $Pd_2Mn_2, Pd_4Mn_2, Pd_8Mn_2$  and  $Pd_{10}Mn_2$ .

The second difference in BE of a particular clusters indicate their relative stability with respect to their neighbors. The peak in the second difference in the bonding energy represents the higher stability of corresponding clusters against breakup. For pristine clusters  $Pd_8$  and  $Pd_{13}$  has higher peaks as in dissociation energy and odd-even alternation is also clear (Rogan et al. 2008, Mosler et al 2001). The mono- and bi-doped clusters also support the results of dissociation energy To verify the chemical stability of the clusters we have to analyze the spin gaps. Spin gaps measure the energy required to move an infinitesimal amount of charge from HOMO of one spin channel to LUMO of the other. The the magnitude of spin gap is a measure of chemical activeness of the clusters. This is shown in the bottom panel of Fig. 3. A large HOMO-LUMO gap implies low chemical reactivity because it is energetically less favorable to add the electrons to higher lying LUMO or extract electrons from a low lying HOMO, thereby prohibiting the formation of a large clusters. So the structure which has larger HOMO-LUMO gap is more stable and vice versa. It is observed that the values of  $\delta_1$  and  $\delta_2$  are positive for all the clusters. These general decrease with increase in clusters size (Zhang et al. 2008). The Fig. 3 indicates that mono-doped clusters have, in general, higher activity than the pristine or bi-doped clusters



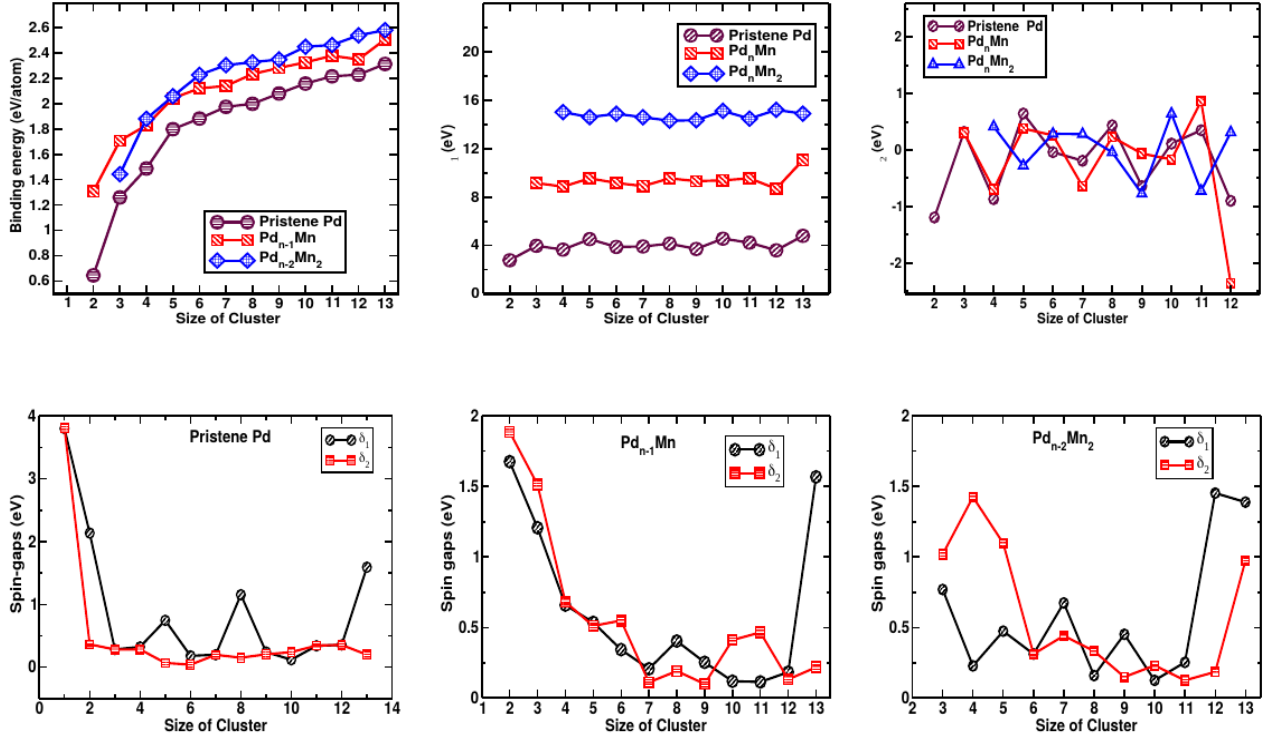


FIG. 3. (Top) Binding energies, first and second energy differences of pristine Pd and mono- and bi-doped Pd clusters (Bottom) spin-gaps (in eV) of (left) pristine Pd (center) mono-doped Pd and (right) bi-doped Pd clusters.

Table I. Summarizes the characteristics of pristine Pd clusters and Pd clusters mono- and bi-doped with Mn.

Pristine Pd Clusters											
Cluster size	Binding Eng.(eV)	Mag.Mom. ( $\mu_B$ )	spin-gap		Avg. bond length ( $\text{\AA}$ )	Cluster size	Binding Eng.(eV)	Mag.Mom. ( $\mu_B$ )	spin-gap		Avg. bond length ( $\text{\AA}$ )
			$\delta_1$ (eV)	$\delta_2$ (eV)					$\delta_1$ (eV)	$\delta_2$ (eV)	
$Pd_2$	0.645	1.214	2.134	0.364	2.48	$Pd_7$	1.974	0.00	0.199	0.197	2.68
$Pd_{22}$	0.654	1.214	0.709	0.709	2.49	$Pd_8$	1.998	5.01	1.1547	0.151	2.67
$Pd_{31L}$	0.859	1.85	0.283	0.148	2.42	$Pd_9$	2.079	1.88	0.242	0.205	2.70
$Pd_{31T}$	1.26	0.00	0.2826	0.2819	2.47	$Pd_{10}$	2.158	1.90	0.119	0.239	2.71
$Pd_4$	1.489	0.00	0.3233	0.2833	2.47	$Pd_{11}$	2.211	5.38	0.3401	0.3451	2.70
$Pd_5$	1.798	1.94	0.745	0.068	2.64	$Pd_{12C}$	2.228	3.82	0.355	0.355	2.69
$Pd_6$	1.882	3.14	1.655	0.034	2.66	$Pd_{13IC}$	2.312	6.87	1.5922	0.1999	2.73
Pd <sub>n</sub> Mn Clusters											
$Pd_1Mn$	0.937	4.91	1.494	1.585	2.30	$Pd_9Mn$	2.325	1.98	0.119	0.411	2.66
$Pd_2Mn$	1.508	5.22	0.400	1.666	2.46	$Pd_{10}Mn$	2.308	3.50	0.146	0.091	2.71
$Pd_3Mn$	1.752	3.93	0.702	0.891	2.47	$Pd_{11}Mn$	2.345	3.67	0.146	0.283	2.72
$Pd_4Mn$	2.004	5.28	0.421	0.555	2.64	$Pd_{12}Mn$ (CUBO)	2.457	2.20	0.013	0.117	2.72
$Pd_5Mn$	2.088	5.27	0.143	0.618	2.66	$Pd_{12}Mn$ (HCP)	2.371	7.00	0.338	0.031	2.71
$Pd_6Mn$	2.135	5.29	0.183	0.257	2.70	$Pd_{12}Mn$ (ICOSA)	2.497	10.0	1.589	0.025	2.69
$Pd_7Mn$	2.232	2.96	0.468	0.147	2.67	$Pd_{12}Mn$ (BBP)	2.460	3.66	0.035	0.802	2.73
$Pd_8Mn$	2.109	7.21	0.459	0.060	2.68						
Pd <sub>n</sub> Mn <sub>2</sub> Clusters											
$Pd_1Mn_2$	1.443	8.74	0.769	1.019	2.49	$Pd_8Mn_2$	2.443	9.35	0.125	0.231	2.68
$Pd_2Mn_2$	1.880	10.00	0.228	1.425	2.51	$Pd_9Mn_2$	2.462	11.01	0.253	0.125	2.66
$Pd_3Mn_2$	2.059	10.00	0.474	1.097	2.47	$Pd_{10}Mn_2$	2.538	12.52	1.453	0.185	2.71
$Pd_4Mn_2$	2.226	9.03	0.312	0.312	2.64	$Pd_{11}Mn_2$ (CUBO)	2.561	1.47	0.134	0.089	2.67
$Pd_5Mn_2$	2.303	10.2	0.674	0.441	2.66	$Pd_{11}Mn_2$ (HPC)	2.477	5.55	0.108	1.062	2.71
$Pd_6Mn_2$	2.326	9.27	0.159	0.333	2.70	$Pd_{11}Mn_2$ (ICO)	2.579	2.00	1.389	0.974	2.69
$Pd_7Mn_2$	2.348	10.71	0.452	0.149	2.67	$Pd_{11}Mn_2$ (BBP)	2.572	2.71	0.429	0.547	2.72

## Magnetic properties

It is well understood that small sized Pd clusters show the magnetic behavior as contrast to the non-magnetic behavior of pure bulk Pd. The actual origin of such a magnetic properties exhibited by such clusters are still unclear. From the study it has been inferred that there is direct effect of bond length between Pd-Pd and Pd-Mn and transfer of charge from Mn sites to Pd. The Fig.5 display the variations of average magnetic moment of Pd and Mn separately, of optimized lowest energy

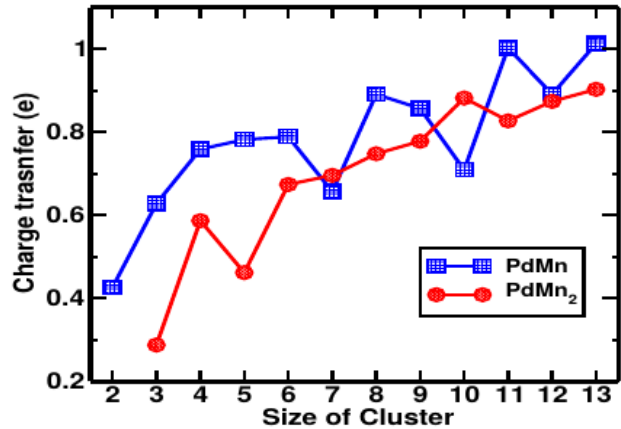
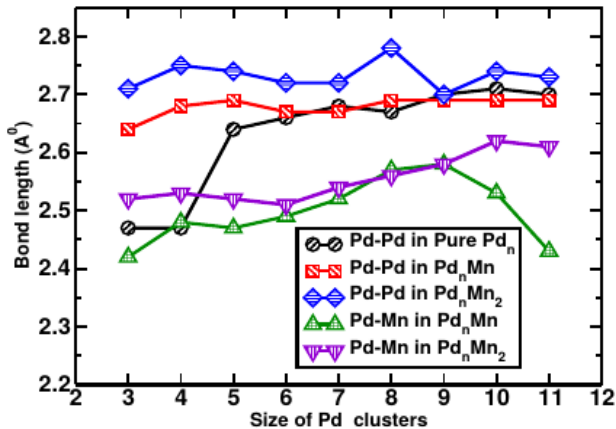


Fig. 4. The (left) average bond-lengths and (right) charge transfers for pristine and doped Pd clusters as functions of cluster size.

configurations of pristine and mono- and bi-doped Pd clusters. The average magnetic moment of Pd behaves more or less step like with the size of Pd clusters within the reference systems whereas the average magnetic moment of Mn found to be decreases monotonically with cluster size except for Pd<sub>6</sub>n and Pd<sub>8</sub>Mn and Pd<sub>9</sub>Mn<sub>2</sub>. These results are resembling with the previously calculated results and developed concepts (Mu et al. 2011; Xi et al. 2023). The magnetic moments also found to be very sensitive with respect to bond length. It is observed that as bond length of Pd-Pd increases magnetic moment of Pd n clusters also increases and vice versa. Longer bond lengths lead to lower hybridization giving higher moments according to the Stoner type argument. But this trend are not strictly followed by pristine clusters of sizes 6,7, 8,10 and 11 atoms. Fig.5 show step like behavior of magnetic moment with size.

In case of mono-doped clusters, there is a slight decrease in magnetic moment of Pd and Mn up to cluster size 6, but nearly same magnetic moment of Pd for n = 7, 8 and 9, whereas one sees high magnetic moment of Mn at n = 7. This may be due to different rates of charge transfer from Mn to Pd. However total magnetic moment of mono-doped clusters is enhanced by 1-7 $\mu$ B as compared with the pristine ones. Bi-doped clusters show even-odd variation for n  $\geq$  6.

Fig. 5 (bottom panel) shows that s-d hybridization dominates the overall properties of these clusters. In case of pristine Pd clusters, Pd 5 clusters show the contribution of p-d hybridization also and produces the local magnetic moments 1.92 $\mu$ <sub>B</sub>. Similarly in case of Pd6 which has a magnetic moments 3.92 $\mu$ <sub>B</sub> and follows the trends dominating s-d hybridization. The maximum magnetic moment is shown at 13-atoms icosahedral structure which is the most stable in this series. The shorter bond lengths of Pd<sub>5</sub> create strong hybridization between the localized d states and p state and hence produce smaller magnetic moment. Whereas for Pd<sub>6</sub> there is significant s-d hybridization offset by

large transitions between up and down spin PDOS which creates its rather larger magnetic moment.

In case of mono-doped clusters there is notable s-d and p-d hybridization which produces large transitions between spin up and down states. Together with sufficient bond lengths it is likely to produce the large magnetic moments. But the relatively smaller bond lengths between Pd-Pd and Pd-Mn in Pd<sub>10</sub>Mn and Pd<sub>11</sub>Mn leads to anti-ferromagnetic alignment between Pd and Mn decreasing the total moments. In the case of Pd<sub>12</sub>Mn the

bond length leads to ferroalignment between Pd and Mn and hence larger total moment.

In the bi-doped clusters we can not totally neglect the p-d contributions. This is due to the unusual magnetic behavior of Mn<sub>2</sub> molecules. The bond lengths between Pd-Pd and Pd-Mn of respective clusters causes the s and d states to split leading to depletion of 4d states through s-p-d hybridization, giving rise to large magnetic moments. Whereas smaller bond lengths create strong d-d interactions and Pd and Mn moments align anti-ferromagnetically. In the icosahedral cluster the two Mn moments also align anti-ferromagnetically as shown in Fig.6.

The knowledge of s-, p- and d-PDOS is required to understand the exact magnetic behavior of the clusters. The PDOS of 13-atoms icosahedral structures for pristine, mono-doped and bi-doped. The Fig.7 indicates strong s-p-d hybridization and that the d-PDOS, exchange split, plays a dominant role in Fig. 6: Magnetic moments (top,left) on Pd in the icosahedral pristine Pd cluster (top,right) on Mn in the BBP Pd<sub>11</sub>Mn<sub>2</sub> cluster (ferrimagnetic), (bottom,left) on Mn in fcc based producing magnetism in these clusters. There is negligible contribution from p-PDOS and an even smaller contribution from s-PDOS. This is consistent with the physical picture that incomplete d-shell electrons should be mainly responsible for the magnetism of TM clusters (Castleman & Jena 2006; Reddy et al. 1993).

## Conclusions

From this study of pristine Pd<sub>n</sub>, Pd<sub>n</sub>Mn and Pd<sub>n</sub>Mn<sub>2</sub> clusters we observed the various interesting features regarding structural, electronic and magnetic properties, which we shall summarize as follows:

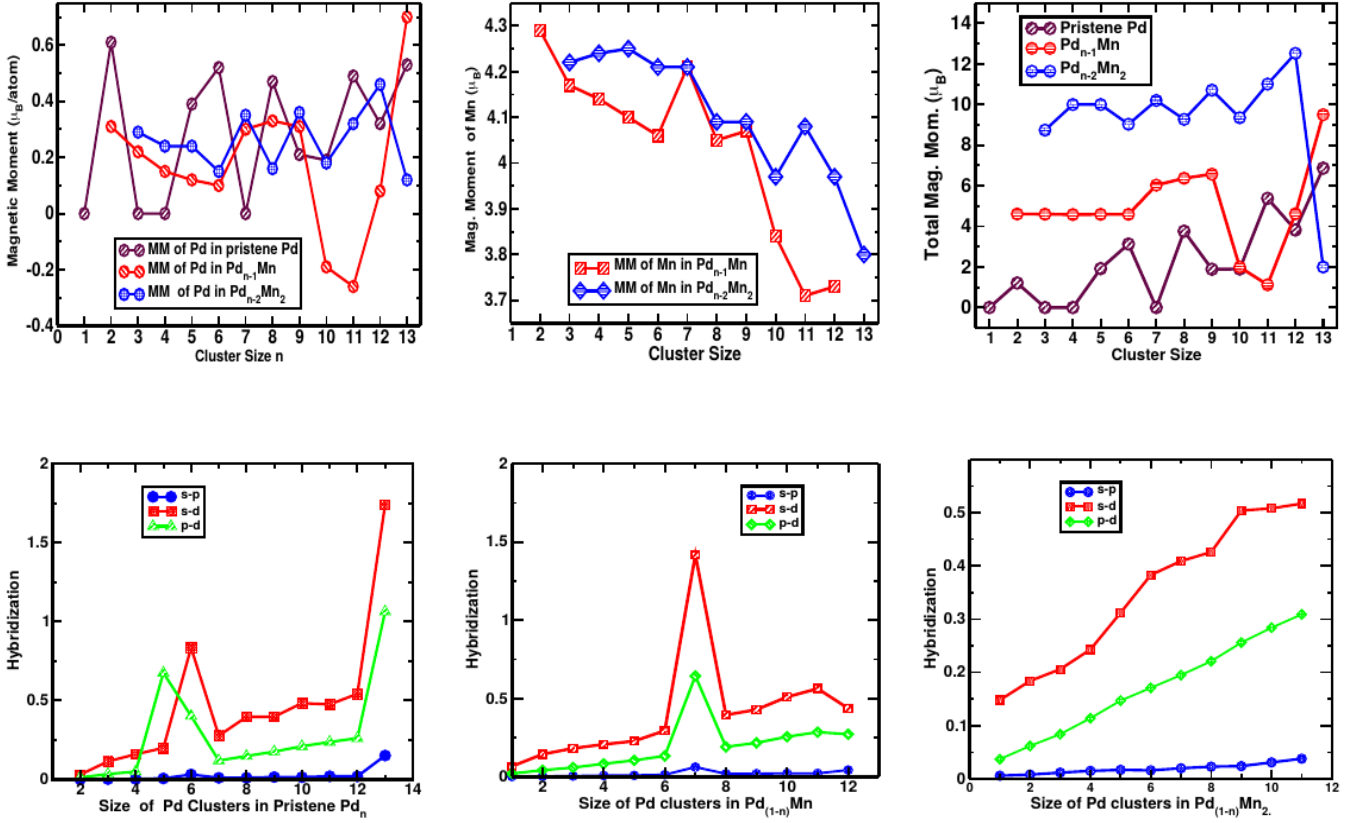


FIG. 5. (Top panel) Average magnetic moment of (left) Pd (center) Mn and (right) total cluster in pristine, mono- and bi-doped Pd clusters. (Bottom panel) Hybridization in (left) pristine (center) mono- and (right) bi-doped Pd clusters.

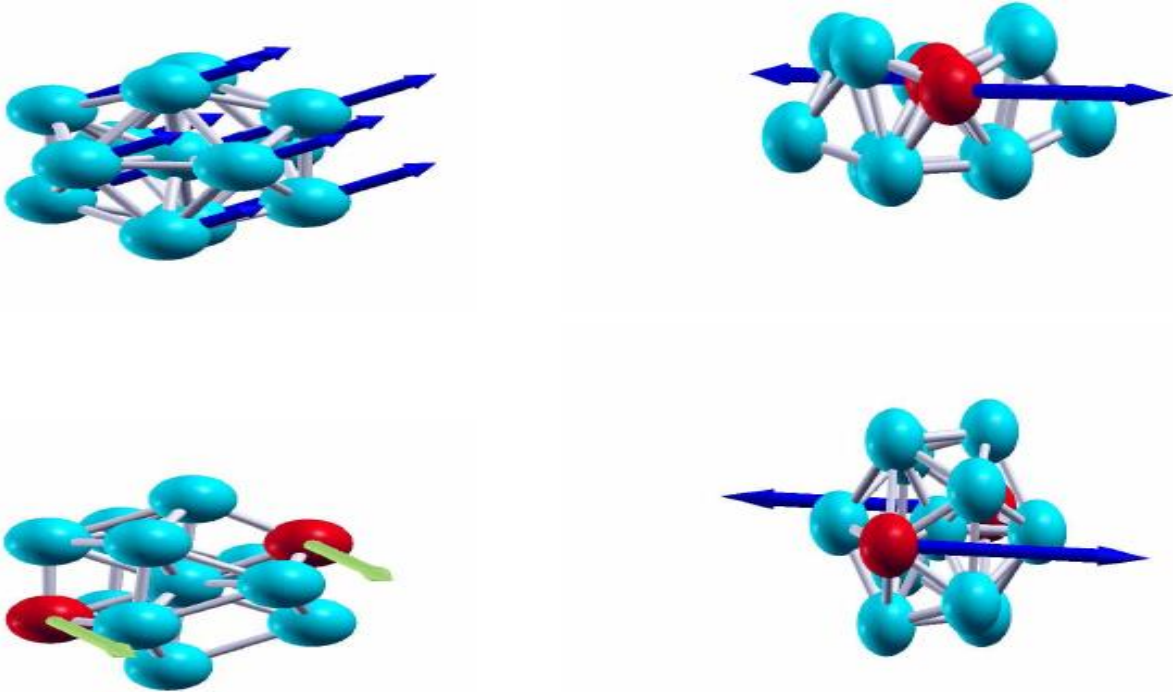


FIG. 6. Magnetic moments (top, left) on Pd in the icosahedral pristine Pd cluster (top, right) on Mn in the BFP  $Pd_{11}Mn_2$  cluster (ferrimagnetic), (bottom, left) on Mn in fcc based  $Pd_{11}Mn_2$  (ferromagnetic) (bottom, right) on Mn in icosahedral  $Pd_{11}Mn_2$  (anti-ferromagnetic).

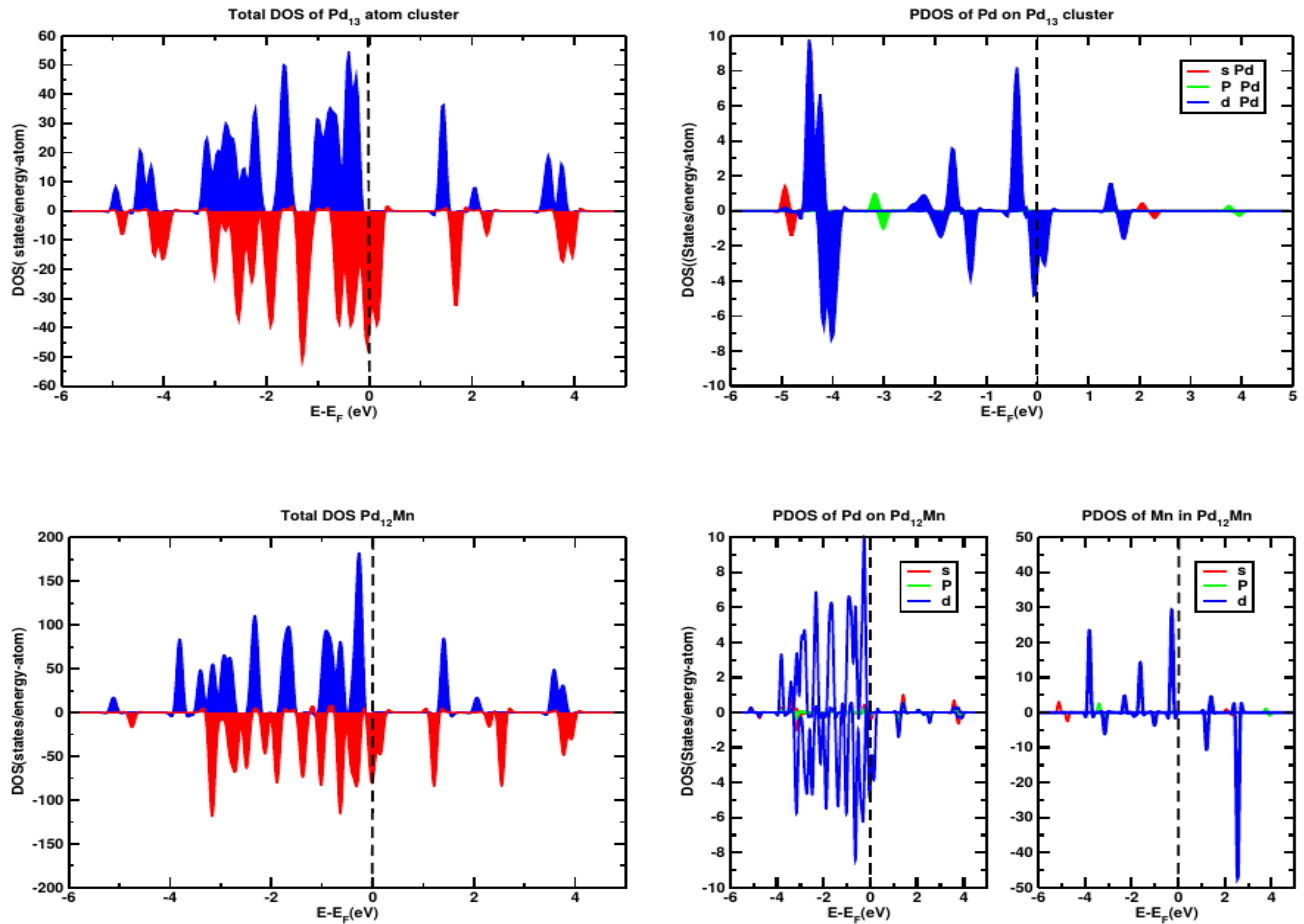


Fig. 7. Total DOS and Spin-orbital projected PDOS for (top) pristine  $Pd_{13}$  (middle)  $Pd_{12}Mn$  (Bottom)  $Pd_{11}Mn_2$

- (i) In general, we notice three types of structural growth motifs (a) fcc based (b) octahedron based and (c) icosahedron based. Of them the icosahedral structure was found to be most stable for 13-atom atoms clusters. This is in contradiction to the buckled biplanar as suggested by some authors. In the bi-doped 13 atom cluster the icosahedral structure has Mn atoms anti-ferromagnetically aligned, while the buckled biplanar has a ferrimagnetic Mn spin alignment. The latter therefore has a higher total magnetic moment than the former.
- (ii) The transition from two dimensional structures to three-dimensional is found between cluster sizes 4, 5 and 6 for pristine and mono-doped Pd, and between 5 and 6 for  $PdMn_2$ .
- (iii) The average binding energy/atom of the clusters increases with increasing the clusters size and tends towards the bulk cohesive energy.
- (iv) The average binding energies of both icosahedral, octahedron and fcc based structures are comparable to that of closed packed "irregular" clusters at  $n = 13$ , indicating that transition from 'irregular' structures to the icosahedral and fcc-like structures could occur at smaller cluster sizes.
- (v) The binding energy per atom and the average bond length of Pd-Pd and Pd-Mn clusters and Bader charges are interlinked with each other. In general binding energy increases with bond length monotonically.
- (vi) The results of dissociation and second differences in the binding energy show that clusters of atoms 2, 8, 13, 18 are clearly found to be more stable than their neighborhoods. The magic number effect is effectively applicable in pristine Pd clusters. The results of HOMO-LUMO gap shows that  $Pd_nMn$  clusters are chemically more reactive than others.
- (vii) Present calculations show that high symmetry, always does not guarantee success when used as a starting point criteria in the search of minimum energy configurations. It is better to carry out unconstrained optimization.
- (viii) A trend of larger magnetic moments with increasing size were not followed but magnetic moment shows odd-even alternation. The magnetic moment was found to be enhanced by  $(3-7)\mu_B$  and  $(2-14)\mu_B$  after doping Mn and  $Mn_2$  on Pd-Pd clusters respectively.
- (ix) Overall cluster structure does not change while doping with one of two Mn atoms, and the lowest-energy structure of  $Pd_{n-1}Mn$  and  $Pd_{n-2}Mn_2$  are also similar to that of  $Pd_n$  clusters. However the magnetic moment of Mn decreases as clusters size increases. This is mainly due to transfer of charge from Mn to Pd and hybridization parameters. There is an intimate relationship between Pd-Pd and Pd-Mn bond lengths; alignment of up and down spin moments and hybridization according to which increasing and decreasing of net magnetic moments of the system occurs.



## Acknowledgement

This work was done under the Hydra collaboration. We are grateful to ICTP/OEA NET-56 program of Trieste, Italy for financial support and SN Bose National Center For Basic Sciences, Kolkata, India for providing computational facility, both made this collaboration successful. One of us GCK acknowledges Dr. Soumendu Datta for providing initial structures of the some clusters.

## References:

- Aguilera-Granja A., Montejano-Carrizales J.M., Berlanga-Ramírez E.O., Vega, A. (2004), Magnetic behaviour of selected geometries of Pd clusters: icosahedral versus fcc structures, *Physics Letters A*, 330(1-2), 126-130.
- Aguilera-Granja F., Balbás L. C., Vega A. (2009). Study of the Structural and Electronic Properties of  $Rh_N$  and  $Ru_N$  Clusters ( $N < 20$ ) within the Density Functional Theory, *J. Phys. Chem. A* **113**, 13483.
- Alonso J. A. (2000), Electronic and Atomic Structure, and Magnetism of Transition-Metal Clusters. *Chem. Rev.* 100, 2, 637-678.
- Bansmann J., Baker S.H., Binns C. et al. (2005). Magnetic and structural properties of isolated and assembled clusters *Surface Science Rep.* 56, 189.
- Blonski P. and Hafner J. (2011), Magneto-structural properties and magnetic anisotropy of small transition-metal clusters: a first-principles study. *J. Phys. Condens. Matter* 23, 136001.
- Boulbazine M. & Boudjahem A. (2023). Stability and electronic sensitivity of  $Cu_nM$  ( $M = Co, Mn, Pd, Au$  and  $V$ ;  $n = 3-8$ ) nanoclusters towards HCOOH molecule: a computational study, *Molecular Physics*, e2237615. DOI: 10.1080/00268976.2023.2237615.
- Castleman A. W. Jr. and P. Jena, (2006) Clusters: a bridge across the disciplines of environment, materials science, and biology, *Proc. Natl. Acad. Sci. U.S.A.* 103, 10554.
- Chang C. M. and Chou M.Y. (2004), Alternative Low-Symmetry Structure for 13-Atom Metal Clusters, *Phys. Rev. Lett* **93**, 133401.
- Chen Z., Neukermans S., Wang Xin *et al* (2006). To Achieve Stable Spherical Clusters: General Principles and Experimental Confirmations. *J. Am. Chem. Soc.* 2006, 128, 39, 12829–12834.
- Douglass D.C., Bucher J. P., and Bloomfield L. A. (1992). Magnetic studies of free nonferromagnetic clusters, *Phys. Rev. B* 45, 6341.
- Grüne O. P., Rayner D. M., Redlich B. et al. (2008). Structures of Neutral  $Au_7$ ,  $Au_{19}$ , and  $Au_{20}$  Clusters in the Gas Phase, *Science* 321, 674 Fig. 6: Magnetic moments (top, left) on Pd in the icosahedral pristine Pd cluster (top, right) on Mn in the BBP  $Pd_{11}Mn_2$  cluster (ferrimagnetic), (bottom, left) on Mn in fcc based.
- Huber K. P. and Herzberg G. (1979), *Molecular Structure and Molecular Spectra IV. Constants of Diatomic Molecules*, Van Nostrand Reinhold, New York.
- Kresse G. and Furthmüller J. (1996). Efficient iterative schemes for *ab initio* total-energy calculations using a plane-wave basis set. *Phys. Rev. B* 54, 11169 (1996).
- Kresse G. and Joubert D. (1999), From ultrasoft pseudopotentials to the projector augmented-wave method, *Phys. Rev. B* 59, 1758.
- Kumar V. and Kawazoe Y. (2002). Icosahedral growth, magnetic behavior, and adsorbate-induced metal-nonmetal transition in palladium clusters, *Phys. Rev. B* 66, 144413.
- Kumar V. (2006). Recent theoretical progress on electronic and structural properties of clusters: Permanent electric dipoles, magnetism, novel caged structures, and their assemblies, *Comput. Mater. Sci.* 35, 375.
- Kumar V and Y. Kawazoe Y. (2003; 2001). Metal-Encapsulated Fullerene-like and Cubic Caged Clusters of Silicon, *Phys. Rev. Lett.* 7, 045503; 91, 199901(E).
- Lee H. W. and Chang C. M. (2011), Size effect of Pd clusters on hydrogen adsorption, *J. Phys. Condens. Matter*, **23**(4), 045503.
- Luo C., Zhou C., Wu J., et al. (2007). First Principles Study of Small Palladium Cluster Growth and Isomerization, *Inter. J. Quantum. Chem.* 107, 1632–1641.
- Massen C., Johnston R. L., Mortimer-Jones T.V. (2002). Geometries and segregation properties of platinum-palladium nanoalloy clusters. *J. Chem. Soc., Dalton Trans.*, 23, 4375-4388.
- Moseler M., Häkkinen H., Barnett R. N., Landman U. (2001), Structure and Magnetism of Neutral and Anionic Palladium Clusters, *Phys. Rev. Lett.* **86**, 2545-2548
- Mu Y., Han Y., Wang J., Wang Jian-guo, and Wang G. (2011). Structures and magnetic properties of Pd<sub>n</sub> clusters (n=3-19) doped by Mn atoms, *Phys. Rev. A* 84, 053201 (2011).
- Nigam S., Majumder C. and Kulshrestha S. K. (2007). Geometry and electronic and magnetic properties of MPd<sub>12</sub> clusters (M=Ti, V, Cr, Mn, Fe, Co, Ni, Cu, Zn, and Pd) from first principles, *Phys. Rev. B* **76**, 195430.
- Perdew J. P., Burke K. and Ernzerhof M., (1996). Generalized Gradient Approximation Made Simple, *Phys. Rev. Lett.* 77, 3865 (1996).
- Piotrowski M. J., Piquini P., and Da Silva J. L. F. (2010). Density functional theory investigation of 3d, 4d, and 5d 13-atom metal clusters. *Phys. Rev. B* **81**, 155446.
- Reddy B. V., Khanna S. N., and Dunlap B. I. (1993). Giant magnetic moments in 4d clusters, *Phys. Rev. Lett.* **70**, 3323
- Reddy B. V., Nayak S.K., Khanna S.N. et al. (1999). Electronic structure and magnetism of  $Rh_n(n=2-13)$  clusters. *Phys. Rev. B* 59, 5214.
- Rogan J., Garcia G., Ramirez M. et al. (2008). The structure and properties of small Pd clusters, *Nanotechnology*, **19** (20), 20570.
- Shinohara T, Sato T, and Taniyama T. (2003). Surface Ferromagnetism of Pd Fine Particles, *Phys. Rev. Lett.* **91**, 197201.
- Taniyama T., Ohta E., and Sato T. (1997). Observation of 4d ferromagnetism in free-standing Pd fine particles, *Europhys. Lett.* 38, 195.
- Walter E. C., Murray B. J., Favier F. et al. (2002). Noble and Coinage Metal Nanowires by Electrochemical Step Edge Decoration, *The Journal of Physical Chemistry B* 106(44), 11407-11411.
- Xi Bai, Yanbin He, Yintao Li, Jin Lv & Haishun Wu (2023). The magnetic anisotropy energy of 13-atom Fe-Pt, Co-Pt and Ni-Pt clusters, *Molecular Physics*. e2249134, DOI: 10.1080/00268976.2023.2249134.
- Zhang H; Tian D.; Zhao J. (2008), Structural evolution of medium-sized Pd<sub>n</sub> (n=15–25) clusters from density functional theory, *J. Chem. Phys.* 129, 114302